A robust solution for the resistive MHD toroidal Δ' matrix in near real-time

Alexander S. Glasser, and Egemen Kolemen

Citation: Physics of Plasmas **25**, 082502 (2018); doi: 10.1063/1.5029477
View online: https://doi.org/10.1063/1.5029477
View Table of Contents: http://aip.scitation.org/toc/php/25/8
Published by the American Institute of Physics

A robust solution for the resistive MHD toroidal Δ' matrix in near real-time

Alexander S. Glasser[1] and Egemen Kolemen[2]
[1]*Department of Astrophysical Sciences, Princeton University, Princeton, New Jersey 08540, USA*
[2]*Princeton Plasma Physics Laboratory, Princeton, New Jersey 08543, USA*

(Received 14 March 2018; accepted 10 July 2018; published online 1 August 2018)

We introduce a new near real-time solution for the tokamak resistive MHD Δ' matrix. By extending state transition matrix methods introduced in [Glasser *et al.*, Phys. Plasmas **25**(3), 032507 (2017)] and leveraging the asymptotic methods of [A. H. Glasser, Phys. Plasmas **23**, 072505 (2016)], we have developed STRIDE—State Transition Rapid Integration with DCON (Asymptotic) Expansions—a code that solves for Δ' in <500 ms. The resistive MHD stability remains a foremost challenge in successful tokamak operation, and its numerically demanding analysis has received attention for many years. Our code substantially improves upon the speed and robustness of earlier Δ' calculation methods, affording solutions for previously intractable equilibria and helping enable the real-time control of ideal and resistive MHD tokamak stability. In this paper, we pedagogically review tearing stability analysis and motivate and define Δ' in the slab, cylindrical, and toroidal geometries. We also benchmark STRIDE against the calculations of [Nishimura *et al.*, Phys. Plasmas **5**, 4292–4299 (1998)] and Furth *et al.* [Phys. Fluids **16**, 1054 (1973)] for Δ' in a cylindrical geometry, and the Δ' matrix calculations of [A. H. Glasser, Phys. Plasmas **23**, 112506 (2016)] in the full toroidal geometry. *Published by AIP Publishing.* https://doi.org/10.1063/1.5029477

I. INTRODUCTION

Resistive magnetohydrodynamic (RMHD) stability remains a foremost challenge in successful tokamak operation. In tokamaks such as JET[6] and DIII-D,[7] neoclassical tearing modes have been shown to degrade tokamak performance by elevating radial transport and, still worse, causing disruptions. At DIII-D, such observations in ITER Baseline Scenario shots raise concerns about the tearing stability of ITER. It is in this context that we address the need for improved tools to analyze tokamaks' RMHD stability.

The RMHD model suggests that plasma resistivity makes little contribution to the stability of magnetic perturbations in tokamaks, except crucially when the magnetic perturbation lies *parallel* to the background magnetic field. In a Fourier decomposition of such a perturbation, this condition corresponds to the perturbation's wavenumber $\mathbf{k}$ lying *perpendicular* to the background field, $\mathbf{k}\cdot\mathbf{B}_0 = 0$. The effects of resistivity on such a perturbation were first analyzed in the study by Furth *et al.*[8] in a slab geometry where it was shown that a first-order magnetic perturbation of the form

$$\mathbf{B}_1(\mathbf{x}) = \mathbf{B}_1(y)\exp\left[i(k_x x + k_z z)\right]e^{\gamma t} \tag{1}$$

can give rise to the tearing mode, opening up "islands" in the magnetic topology.

This analysis was later generalized to curvilinear geometries. In a toroidal geometry, for example, the Fourier perturbation $\exp\left[i(m\theta + n\phi)\right]$ has an angular wavenumber characterized by its poloidal and toroidal mode numbers (m, n), respectively. The $\mathbf{k}\cdot\mathbf{B}_0 = 0$ condition has the toroidal analog $q = m/n$, where the safety factor q—defined as the relative pitch angle of magnetic lines of force, $q \equiv \frac{d\phi}{d\theta}$—takes rational values. Since modes of low toroidal number n are generally the most unstable and since q spans a finite range over the plasma profile—$1 < q < 10$ for most tokamak profiles—it is common to explore primarily the finite set of Fourier modes (m, n) for which low-n rational surfaces $\{\psi^* \,|\, q(\psi^*) = m/n,\ n \gtrsim 1\}$ appear in the plasma profile.

The *localized* importance of resistivity near such rational surfaces suggests two feasible approaches toward the analysis of tearing mode stability in tokamaks: (i) The first approach is taken by codes—such as MARS[9]—that solve the full RMHD equations over the entirety of the plasma profile. This technique has the benefit of solving the full physical equations everywhere but is limited in scope to calculating a single stability eigenvalue at a time; it also has difficulty resolving *stable* eigenvalues due to the continuous MHD spectrum in the stable range. The latter feature limits its utility in control applications, in particular where a measure of the "distance-to-instability-boundary" may be useful in the analysis of stable equilibria.[1] (ii) The second, "external/internal region" approach, is taken by codes—such as resistive DCON[5]—that treat the rational surfaces as effective boundary layers. In particular, resistive DCON ignores the negligible plasma resistivity in "external regions" (far from the singular surfaces) by solving the *ideal* MHD equations in those regions. It then asymptotically matches the ideal MHD external solutions to "inner region" RMHD solutions, which are solved only very near the singular surfaces.

The latter approach, analyzed in depth for the toroidal case in the study by Glasser *et al.*,[10] simultaneously solves for the stability eigenvalues of all perturbed modes of a given profile (truncated at some $n \gtrsim 1$ and some large m). It has the advantages of speed and wide-spectrum information, which make this approach particularly suitable for active feedback control of tokamak plasmas. This method has the drawback of requiring asymptotic matching, which can be especially challenging in low-β regions of the plasma—such

as the tokamak edge.[5] The difficulty of generating accurate asymptotic expansions in low β, often referred to as the "overlap problem," is a subject of active research.

Historically, the "external/internal region" approach of codes such as resistive DCON was the first used to conduct tearing stability analysis, appearing alongside the discovery of the tearing mode by Furth *et al.* in Ref. 8. That work introduced the Δ' parameter in the slab model as an asymptotic matching criterion—a parameter derived by solving the external region equations and used as boundary constraints for the inner region solution. As we will discuss at length in Sec. II, in a tokamak geometry, the corresponding Δ' *matrix* is, similarly, a characterization of asymptotic matching criteria found by solving the external region equations.

Given its appropriateness to our purposes, we will pursue the "external/internal region" approach to tearing stability analysis in the remainder of this paper and improve upon known methods by introducing a state transition matrix solution for Δ'. A robust solution for the Δ' boundary value problem (BVP) in the external regions of a toroidal geometry has remained an open challenge for many years. The singularity of the ideal MHD equations at a tokamak's rational surfaces, and their stiffness particularly near the magnetic axis,[2] make the external solutions to the ideal MHD equations quite numerically challenging.

In a cylindrical geometry, Nishimura *et al.*[3] solved the external regions by a shooting method that shot outward and away from the rational surface, attempting to satisfy boundary conditions at the magnetic axis and plasma edge. In that work, the BVP solution was achieved by a Newton iteration, which iteratively reduced the error of the shot's boundary conditions until convergence. While effective for most cylindrical equilibria, this iterative method has two notable limitations:

- First, it does not seize upon the linearity of the ideal MHD differential equations. If enough shots are simultaneously taken to span the finite solution space of a *linear* ordinary differential equation (ODE)—and this is only two shots in the cylindrical ideal MHD case—a viable solution will exist as a linear combination of the resulting integrations, obviating the less robust iteration. Linearity furthermore affords a *decomposition* of the domain of integration, as described in Ref. 1, allowing for its parallelized, rapid solution.
- Second, the shot outward from a single rational surface is limited to a cylindrical geometry; the presence of multiple singular surfaces and the coupling of Fourier modes in the tokamak geometry unavoidably multiply the required number of shots.

In the full toroidal geometry, resistive DCON[5] has more recently approached the challenge of solving the external ideal MHD regions via a Galerkin expansion, as first suggested in Ref. 11 and adapted in Refs. 12 and 13. While effective in most cases, Galerkin expansions by their nature cover only a (finite element) subspace of the possible solution space, which limits their accuracy as compared to direct integration methods—especially for singular ODEs. Furthermore, known implementations for the Galerkin method in the external regions do not guarantee the existence of solutions for ideal-MHD-unstable plasmas, limiting their usefulness in high-throughput real-time stability analysis—as we will discuss in Sec. V.

In this paper, we thoroughly address the above limitations and develop a solution for Δ' in cylindrical and toroidal geometries which is *fast* and *robust*. The `STRIDE` code extends the state transition matrix Riccati techniques introduced in Ref. 1 for ideal MHD stability calculations. `STRIDE` makes abundant use of the linearity of the ideal MHD equations to divide the Δ' BVP integration into subintervals, associating to each its fundamental matrix of solutions. It integrates *away* from all singular surfaces and stitches together ODE solutions by enforcing continuity criteria at each subinterval interface. It then solves these continuity and boundary conditions simultaneously as a large sparse matrix problem, rendering the Δ' BVP as an algebraic equation.

The resulting solution provides the external region matching criteria for "resonant" modes at singular surfaces—precisely the information stored in the Δ' matrix. `STRIDE` avoids a costly Newton iteration, leverages the linearity of the ODE to "shoot" (a linearly complete set of modes) once on each subinterval, and sidesteps a Galerkin expansion which may be ill-posed for ideal-MHD-unstable equilibria. We will show that the parallelized, state transition matrix integration of the complete solution space affords greater robustness and speed than previously known approaches.

The remainder of this paper is organized as follows: In Sec. II, we review at length the definitions of Δ' in the slab, cylindrical, and toroidal contexts. In Sec. III, we extend the techniques of Ref. 1 to develop a solution method for the cylindrical geometry Δ', comparing our results with Refs. 3 and 4. In Sec. IV, we complete this development to solve the full toroidal Δ' matrix problem with our `STRIDE` code; we compare our method's results against those of resistive DCON.[5] In Sec. V, we discuss numerical advantages of `STRIDE` and some limitations of the Galerkin approach. In Sec. VI, we discuss our conclusions.

II. A BRIEF REVIEW OF Δ' IN TEARING MODE STABILITY ANALYSIS

A. The slab geometry Δ' of Furth *et al.*

The Δ' parameter was first introduced by Furth *et al.*[8] in a plasma slab geometry, for which the background magnetic field $\mathbf{B}_0(\mathbf{x}) = \hat{x}B_{x0}(y) + \hat{z}B_{z0}(y)$ has only y-dependence. That work considered a first order magnetic perturbation of the RMHD equations, given by

$$\frac{\partial \rho}{\partial t} + \nabla \cdot (\rho \mathbf{v}) = 0, \tag{2}$$

$$\rho \frac{d\mathbf{v}}{dt} = \mathbf{J} \times \mathbf{B} - \nabla p, \tag{3}$$

$$\frac{\partial \mathbf{B}}{\partial t} = \nabla \times (\mathbf{v} \times \mathbf{B}) + \frac{\eta}{\mu_0} \nabla^2 \mathbf{B}, \tag{4}$$

$$\frac{d}{dt}\left(\frac{p}{\rho^{\gamma}}\right) = 0. \tag{5}$$

We recall the definition of the dimensionless Lundquist number

$$S \equiv \frac{\tau_R}{\tau_A} \equiv \frac{\left(a^2/\frac{\eta}{\mu_0}\right)}{(a/v_A)} = \frac{a v_A}{\eta/\mu_0}, \tag{6}$$

where a is the plasma width, η is the plasma resistivity, and $v_A \equiv \frac{B}{\sqrt{\mu_0 \rho}}$ is the Alfvén velocity. In the (ideal MHD) $S \to \infty$ and $\omega\tau_A \ll 1$ limit—after introducing a slab perturbation in the form of Eq. (1) and taking $\beta \equiv \frac{p}{B^2/2\mu_0} = 0$—it can be demonstrated that the linearized RMHD equations reduce to an ideal MHD equation for the perturbed mode with wavenumber $\mathbf{k}$

$$B_{y1}'' - \left(k^2 + \frac{F''}{F}\right) B_{y1} = 0, \tag{7}$$

where primes denote derivatives with respect to the y coordinate and where $F \equiv F(y) \equiv \mathbf{k} \cdot \mathbf{B}_0$. This equation is specific to a single mode $\mathbf{k}$, indicating that perturbed modes are decoupled in the slab model for ideal MHD.

$S \approx 10^7$ in a typical tokamak, and so, the ideal MHD Eq. (7) holds to high accuracy everywhere in the plasma, except where the equation is singular.[13,14] We see that a singularity occurs at y^* when $F(y^*) = 0$; this is an indication that in a layer near the singularity, the simplified ODE is nonphysical, and a full resistive treatment is required to solve for the magnetic perturbation.

At a finite distance ϵ from this layer at the singularity, we may solve Eq. (7) as follows: Boundary conditions are imposed at some distance on either side of y^*

$$B_{y1}|_{y=\pm a} = 0, \tag{8}$$

and the two outer regions $(-a, y^* - \epsilon)$ and $(y^* + \epsilon, a)$ may be solved independently. The two solutions are found to have a discontinuous jump in their derivatives at y^*, which is used to define

$$\Delta' \equiv \lim_{\epsilon \to 0} \frac{B_{y1}'(y^* + \epsilon) - B_{y1}'(y^* - \epsilon)}{B_{y1}(y^*)} = \lim_{\epsilon \to 0} \left[\frac{B_{y1}'}{B_{y1}}\right]_{y^*-\epsilon}^{y^*+\epsilon}. \tag{9}$$

As we next show, this Δ' parameter stores the information which must be taken from the *outer* solution to determine the tearing stability of the slab model.

In the slab model, the *inner* layer may be approached by assuming the simplest model of plasma resistivity—setting η constant in the induction equation, as in Eq. (4). The first order perturbation of the y component of Eq. (4) can be integrated to find an inner layer solution that asymptotically satisfies the value of Δ' in Eq. (9). In particular, denoting the inner layer perturbed solutions by $\tilde{\mathbf{B}}_1$ and $\tilde{\mathbf{v}}_1$ and noting that the Laplace operator is dominated by the variation in y near the singularity, asymptotic matching is achieved by requiring that

$$\frac{\eta}{\mu_0}\Delta' \sim \frac{\eta}{\mu_0}\left[\frac{\tilde{B}_{y1}'}{\tilde{B}_{y1}}\right]_{-\infty}^{+\infty} \approx \frac{1}{\tilde{B}_{y1}} \int_{-\infty}^{+\infty} \left[\gamma \tilde{B}_{y1} - (i\mathbf{k} \cdot \mathbf{B}_0)\tilde{v}_{y1}\right] dy, \tag{10}$$

where we have set $\nabla \times (\mathbf{v} \times \mathbf{B}) \approx (\mathbf{B}_0 \cdot \nabla)\mathbf{v}_1$ and where $\sim$ indicates asymptotic agreement in the limit that the outer region solutions approach y^* and the inner region solutions extend to $\pm\infty$. (Although its derivative $\tilde{B}_{y1}'$ varies considerably over the inner region, $\tilde{B}_{y1}$ may be treated as constant in the inner region.) The first (asymptotic) equality of Eq. (10) demonstrates how the Δ' parameter sets the asymptotic *matching criteria* for the inner layer equation in the slab model.

The RMHD equations can be used to solve for $\tilde{B}_{y1}$ and $\tilde{v}_{y1}$ in the expression above. Under the assumptions of a narrow resistive layer and plasma incompressibility (i.e., $\nabla \cdot v_1 = 0$), one finds that Eq. (10) can be solved for γ—the growth rate of the tearing mode, whose sign dictates the mode's stability. It turns out[15] that $\text{sign}(\Delta') = \text{sign}(\gamma)$, and indeed, γ is given by

$$\gamma = \frac{0.55(\Delta' a)^{4/5}}{\tau_A^{2/5}\tau_R^{3/5}}, \tag{11}$$

where the characteristic Alfvénic and resistive timescales τ_A and τ_R, respectively, are defined in Eq. (6). In summary, the tearing modes of the slab model are decoupled in the sense that their governing equations are independent of one another. In particular, for each mode of wavenumber $\mathbf{k}$ for which a singular point exists in the plasma ($\mathbf{k} \cdot \mathbf{B}_0 = 0$), there is an associated stability parameter $\Delta'(\mathbf{k})$ determined solely by this mode. $\Delta'(\mathbf{k})$ is furthermore in one-to-one correspondence with the growth rate of the mode—γ—sharing its sign and crossing zero at the same time. This decoupling between modes, and the direct relationship between Δ' and tearing stability, are features of the slab model that persist in a cylindrical geometry. As we shall see, however, these features will no longer hold in the toroidal case.

B. The cylindrical Δ'

The cylindrical analog of Eq. (7) is given by the ideal MHD Newcomb equation[3,4,16]

$$\begin{pmatrix} \psi \\ \psi' \end{pmatrix}' = \begin{pmatrix} 0 & 1 \\ \frac{1}{H}\left[\frac{g}{F^2} + \frac{1}{F}(HF')'\right] & -\frac{H'}{H} \end{pmatrix} \begin{pmatrix} \psi \\ \psi' \end{pmatrix}, \tag{12}$$

where $B_{r1} = \psi(r)\exp[\omega t + i(k_z z + m\theta)]$ represents a radial magnetic perturbation, primes are derivatives with respect to the radial coordinate r, and

$$\begin{aligned} F(r) &\equiv \mathbf{k} \cdot \mathbf{B}_0 = k_z B_z + \left(\frac{m}{r}\right) B_\theta \equiv \frac{B_z}{R_0}\left(n - \frac{m}{q}\right) \\ H(r) &\equiv \frac{r^3}{k_z^2 r^2 + m^2} \\ g(r) &\equiv \frac{(m^2 - 1) r F^2}{k_z^2 r^2 + m^2} + \frac{k_z^2 r^2}{k_z^2 r^2 + m^2} \\ &\quad \times \left(rF^2 + rF\frac{2\left(k_z B_z - \frac{m}{r}B_\theta\right)}{k_z^2 r^2 + m^2} + 2\mu_0 \frac{dp}{dr}\right). \end{aligned} \tag{13}$$

As in the slab model, this ideal MHD equation is given for a single, decoupled mode (m, n) and is singular when $F(r^*) = 0$, that is, where $q(r^*) = m/n$. (Note that

$$q(r) \equiv \frac{-rB_z(r)}{R_0 B_\theta(r)} \tag{14}$$

in cylindrical geometry, and we have implicitly taken $k_z \equiv \frac{n}{R_0}$ above.) As in the slab model, we impose Dirichlet boundary conditions

$$\psi(0) = \psi(2a) = 0, \tag{15}$$

where $r = 2a$ is the plasma edge. (a can be regarded as a characteristic lengthscale of the problem; here, it is just a half-radius.)

Because the cylindrical Newcomb equation is unimodal, it would suffice to continue describing Δ' as a scalar parameter in the cylindrical case, as we did in the slab model. As preparation for the toroidal Δ' matrix, however, we instead find it instructive to define a cylindrical Δ' matrix in the discussion that follows.

We must first examine the asymptotic solutions of our ODE near its singular point r^*. Leading order terms of the ODE in Eq. (12) form a simpler asymptotic ODE near r^*. For ease of presentation, we assume a pressureless $\beta = 0$ cylindrical plasma. Letting primes denote derivatives with respect to the dimensionless parameter $s \equiv \frac{r-r^*}{a}$, this leading order ODE is given by

$$\psi'' - \frac{\kappa}{s}\psi = 0, \tag{16}$$

where the constant $\kappa = \lim_{s\to 0}(a^2 s) \cdot \frac{1}{H}\left[\frac{g}{F^2} + \frac{1}{F}(HF')'\right]$. This ODE is easy to solve with a Frobenius expansion, yielding the following asymptotic solutions for the full ($\beta = 0$) ODE Eq. (12) at the singular surface r^*[3]

$$\begin{aligned} \psi_B(r) &\sim 1 + \kappa s \ln|s| + \frac{1}{2}\kappa^2 s^2 \ln|s| - \frac{3}{4}\kappa^2 s^2 + \cdots, \\ \psi_S(r) &\sim s + \frac{1}{2}\kappa s^2 + \frac{1}{12}\kappa^2 s^2 + \cdots. \end{aligned} \tag{17}$$

These solutions are termed the "big" and "small" solutions, respectively, due to their behavior as $s \to 0$. At a distance $s = \pm\delta$ from the singular surface, the asymptotic expansions provide "initial conditions" for Eq. (12) on either side of the singular surface

$$\left\{ \begin{pmatrix} \psi_B \\ \psi_B' \end{pmatrix}(\pm\delta) \sim \begin{pmatrix} 1 \pm \kappa\delta \ln|\delta| \\ \kappa(\ln|\delta| + 1) \end{pmatrix}, \quad \begin{pmatrix} \psi_S \\ \psi_S' \end{pmatrix}(\pm\delta) \sim \begin{pmatrix} \pm\delta + \frac{1}{2}\kappa\delta^2 \\ 1 \pm \kappa\delta \end{pmatrix} \right\}. \tag{18}$$

Given the linearity of the ODE, the full BVP is solved independently on the left and right sides of the rational surface by some linear combination of the two solutions. The asymptotic expansions therefore provide a linearly independent set of initial conditions at (a small distance from) the singular surface, whose integrations out to the boundaries form a complete basis for the ODE solutions. We denote these solutions on either side of r^* by

$$\begin{aligned} \psi(r < r^*) \equiv \psi_L(r) &= A_L\psi_S(r) + B_L\psi_B(r) \\ \psi(r > r^*) \equiv \psi_R(r) &= A_R\psi_S(r) + B_R\psi_B(r). \end{aligned} \tag{19}$$

It is instructive to count the degrees of freedom (DOF) that must be determined to solve this BVP. The coefficients $\{A_L, A_R, B_L, B_R\}$ constitute four DOF in the BVP, and two of these are determined by the boundary conditions at $\{\psi = 0, \psi = 2a\}$. This leaves two DOF undetermined. The ambiguity of these two remaining DOF (which arises from the discontinuity of our ODE at its singular point) is resolved by storing matching data for our asymptotic solutions in Δ', as we now describe.

To span the remaining two "dimensions" of our BVP solution space (and thereby allow for the most general possible inner layer solutions), we examine two linearly independent assignments for the big solution coefficients

$$\begin{pmatrix} B_L \\ B_R \end{pmatrix} \in \left\{ \begin{pmatrix} 1 \\ 0 \end{pmatrix}, \begin{pmatrix} 0 \\ 1 \end{pmatrix} \right\}. \tag{20}$$

Assigning the big solution coefficients to one vector or the other in Eq. (20), we solve the BVP for the remaining coefficients $\{A_L, A_R\}$ that satisfy the boundary conditions at the axis and plasma edge. In this way, we define the Δ' *matrix* as

$$\Delta'_{ij} \equiv \left(A_j \,|\, B_k = \delta_{ik} \text{ and } \psi(0) = \psi(2a) = 0\right), \tag{21}$$

where $i, j, k \in \{L, R\}$.

In short, row i of this 2×2 Δ' matrix describes the small solution coefficients necessary to solve the BVP when the coefficient of big solution i is set to 1 and the other is set to 0. We have thus resolved the two ambiguous DOF of our BVP simply by solving two linearly independent assignments of these DOF. The information describing the relationships of the big and small solutions for each independent assignment is then stored in each row of the Δ' matrix.

As described in Ref. 13, in the cylindrical model, this definition of Δ' turns out to be a rather trivial extension of our earlier definition Eq. (9). In particular, the left and right side BVPs are independent of one another, such that the 2×2 cylindrical Δ' matrix is diagonal. It contains little more information than it would had when we simply continued to define Δ' as in Eq. (9). [Note that Eq. (9) implicitly sets $B_L = B_R = 1$ and defines $\Delta' = A_R - A_L$.] However, defining the cylindrical Δ' in this way is pedagogically useful, as it makes the toroidal Δ' a natural extension.

We will not pursue the dispersion relation of the cylindrical tearing mode here nor discuss the asymptotic matching in its derivation. Suffice it to say that, as in Eq. (11) of the slab model, there is a one-to-one correspondence in the sign of γ with Δ', and Δ' is a straightforward indicator of tearing mode stability as a result.

C. The toroidal Δ'

The mathematical description of the toroidal tearing mode is rather more involved, and a formidable derivation of

its dispersion relations [analogous to Eq. (11) above] can be found in Ref. 10. For our present purposes, we note that the toroidal analog of the ideal MHD Eq. (7) is given by a matrix Newcomb equation

$$(\mathbf{F}\Xi' + \mathbf{K}\Xi)' - (\mathbf{K}^\dagger \Xi' + \mathbf{G}\Xi) = 0 \tag{22}$$

—see Eq. (21) of Ref. 2—where primes are derivatives with respect to the radial coordinate ψ, and the ψ-dependent matrices $\{\mathbf{F} = \mathbf{F}^\dagger, \mathbf{G} = \mathbf{G}^\dagger, \text{and } \mathbf{K} \neq \mathbf{K}^\dagger\} \in C^{M\times M}$ represent the physics associated with the ideal plasma response to the plasma displacement $\boldsymbol{\Xi}$, where $\boldsymbol{\Xi} \in C^{M\times 1}$ is a vector of Fourier amplitudes for a (truncated) series of (m, n) modes comprising a radial perturbation. (Note that this *independent* variable use of ψ as a spatial coordinate stands in contrast to the *dependent* variable it represents as a magnetic perturbation in the cylindrical case.) We note immediately that these (non-diagonal) matrices couple the various Fourier modes in the toroidal model's ODE.

To assess the singular behavior of this ODE, we note from Eq. (29) of Ref. 2 that the matrices can be rewritten as $\{\mathbf{F} = \mathbf{Q}\bar{\mathbf{F}}\mathbf{Q}, \mathbf{K} = \mathbf{Q}\bar{\mathbf{K}}, \text{and } \mathbf{G} = \bar{\mathbf{G}}\}$, where the barred matrices are nonsingular and $\mathbf{Q}$ is defined as

$$Q_{m,m'}(\psi) \equiv (m - q(\psi)n)\cdot \delta_{m,m'}. \tag{23}$$

[For notational ease, we treat the ordering of modes here as if n is some integer constant and $m = (1, \ldots, M)$. This does not exclude an analysis with multiple n's and $m \leq 0$ but simplifies the presentation.] Rewriting Eq. (22) as a $2M \times 2M$ Hamiltonian system, where $\mathbf{q} \equiv \boldsymbol{\Xi}$ and $\mathbf{p} \equiv (\mathbf{F}\boldsymbol{\Xi}' + \mathbf{K}\boldsymbol{\Xi})$, then emphasizes the ODE's singularities

$$\begin{pmatrix}\mathbf{q}\\ \mathbf{p}\end{pmatrix}' = \left(\begin{array}{c|c} -\mathbf{Q}^{-1}\bar{\mathbf{F}}^{-1}\bar{\mathbf{K}} & \mathbf{Q}^{-1}\bar{\mathbf{F}}^{-1}\mathbf{Q}^{-1} \\ \hline \bar{\mathbf{G}} - \bar{\mathbf{K}}^\dagger\bar{\mathbf{F}}^{-1}\bar{\mathbf{K}} & \bar{\mathbf{K}}^\dagger\bar{\mathbf{F}}^{-1}\mathbf{Q}^{-1}\end{array}\right)\begin{pmatrix}\mathbf{q}\\ \mathbf{p}\end{pmatrix}. \tag{24}$$

Each rational surface $\{\psi^* \,|\, q(\psi^*) = m/n\}$, where the diagonal matrix $\mathbf{Q}$ loses full rank, evidently causes singular behavior in two of the $2M$ linearly independent solutions to this Hamiltonian system—in some vector component labeled by q_s and its conjugate momentum p_s. [Note using Eq. (24) that the ℓth Fourier mode can be removed from the analysis by deleting the ℓth and $(\ell + M)$th rows of the above matrix equation, so that singular pairs q_s and p_s are always separated by M indices.] It will be useful to have a compact notation for the toroidal Newcomb equation, Eq. (24)

$$\mathbf{u}' = \mathbf{L}\mathbf{u}, \text{ where } \mathbf{u} \equiv \begin{pmatrix}\mathbf{q}\\ \mathbf{p}\end{pmatrix} \in C^{2M}. \tag{25}$$

The $2M$ asymptotic solutions at the singular (rational) surfaces of Eq. (25) are worked out in Ref. 2, Eqs. (30)–(47) via a matrix Frobenius method due by Turrittin.[17] We will not repeat that analysis here, but its results are easily described. We let ψ^* denote one such singular rational surface. Then, as $\psi \to \psi^*$, the $(2M-2)$ "nonresonant" (i.e., nonsingular) asymptotic solutions scale as $(\psi - \psi^*)^0 \sim 1$. In fact, they approach the orthonormal basis spanning the $(2M-2)$-dimensional "nonresonant subspace" at the singular surface

$$\lim_{\psi\to\psi^*}[\mathbf{u}_\ell(\psi)]_k = \delta_{\ell k}, \tag{26}$$

where $0 \leq \ell, k \leq 2M$ and $\ell \notin \{s, s+M\}$. Here, $\mathbf{u}_\ell(\psi) \in C^{2M}$ is one of the $(2M-2)$ nonresonant modes in the neighborhood of ψ^*, identified by the index—ℓ—of the mode's nonvanishing component at ψ^*. s is the index of the singular Fourier mode at ψ^*. $[\mathbf{u}_\ell(\psi)]_k$ is the kth element of the $2M$-component vector $\mathbf{u}_\ell(\psi)$.

As $\psi \to \psi^*$, the remaining two "resonant" modes scale as $(\psi - \psi^*)^{-\frac{1}{2}\pm\sqrt{-D_I}}$, where D_I is the toroidal Mercier criterion.[18] For most (ideal-MHD-stable) toroidal geometries, $D_I < -\frac{1}{4}$, so that the resonant modes again split into "small" and "big" solutions, with the former having vanishing norm as $\psi \to \psi^*$ and the latter now having *infinite* norm in the same limit. The big solution corresponds to a mode with the infinite q_s component at ψ^*, $q_s(\psi^*) = \infty$ and the small solution to a mode with the vanishing p_s component, $p_s(\psi^*) = 0$. We may therefore represent the two resonant solutions as

$$\lim_{\psi\to\psi^*}[\mathbf{u}_s(\psi)]_k = \delta_{sk}\cdot\infty\,, \quad \lim_{\psi\to\psi^*}[\mathbf{u}_{s+M}(\psi)]_k = 0. \tag{27}$$

In summary, the set of all $2M$ asymptotic expansions, when mapped to $\psi = \psi^*$, looks like the columns of the following $2M \times 2M$ diagonal matrix:

$$\lim_{\psi\to\psi^*}\mathbf{U}(\psi) = \begin{bmatrix} 1_{s-1} & & & & \\ & \infty & & & \\ & & 1_{M-1} & & \\ & & & 0 & \\ & & & & 1_{M-s}\end{bmatrix}, \tag{28}$$

where 1_n represents the $n \times n$ identity matrix and $\mathbf{U}(\psi)$ is the fundamental matrix of solutions in the neighborhood of ψ^* with columns given by $\{\mathbf{u}_\ell\}$.

Note that, because the toroidal Hamiltonian system couples all modes, all of the $2M$ modes asymptotically expanded at some distance ϵ away from ψ^* are nonzero in every vector component. However, as if we somehow managed to integrate our singular ODE all the way to the singularity, we note that such a mode at $\psi = \psi^* \pm \epsilon$ maps at $\psi = \psi^*$ to one of the matrix columns of Eq. (28)—with only one nonzero component (if any). In this sense, the asymptotic expansion stands in as a method of integration for our ODE in the singular intervals $\psi \in [\psi^* - \epsilon, \psi^*]$ and $\psi \in [\psi^*, \psi^* + \epsilon]$, as if initialized at $\psi = \psi^*$ with the singular matrix columns of Eq. (28).

Having described the asymptotic expansions at a rational surface of a toroidal equilibrium, we can now define the BVP whose solutions produce Δ' in toroidal geometry. We impose the following boundary conditions on each subinterval:

$$\begin{aligned}
\mathbf{q}(\psi_{\text{axis}}) &= 0\\
\mathbf{q}(\psi_{\text{edge}}) &= 0\\
\lim_{\delta\to 0}\begin{pmatrix}\mathbf{q}\\ \mathbf{p}\end{pmatrix}(\psi_s - \delta) &= \lim_{\delta\to 0}\begin{pmatrix}\mathbf{q}\\ \mathbf{p}\end{pmatrix}(\psi_s + \delta), \quad \forall\ \{q_j \neq q_s, p_j \neq p_s\}\\
\lim_{\delta\to 0}\begin{pmatrix}\mathbf{q}\\ \mathbf{p}\end{pmatrix}(\psi_i - \delta) &= \lim_{\delta\to 0}\begin{pmatrix}\mathbf{q}\\ \mathbf{p}\end{pmatrix}(\psi_i + \delta), \quad \forall\ \{q_j, p_j\}.
\end{aligned} \tag{29}$$

In the above, ψ_s and ψ_i reflect the $2M-2$ boundary conditions specified on each singular surface, and $2M$ boundary conditions specified on each "interstitial" surface, respectively. (See Fig. 1.)

We treat the general case of N singular surfaces $\{\psi_1,\ldots,\psi_N\}$, which divide $[0,1]$ into $N+1$ subintervals. We split every interval in half again, creating a total of $2N+2$ subintervals, such that only one side of each subinterval is a singular surface or boundary. It is convenient to label these intervals interchangeably as $i\in\{R_{\text{axis}},L_1,R_1,\ldots,L_N,R_N,L_{\text{edge}}\}$ or $i\in\{1,\ldots,2N+2\}$.

As we defined ψ_L and ψ_R in the cylindrical case, we define the function $\mathbf{u}^i$ as representing the BVP solution on the ith subinterval of the toroidal model and vanishing elsewhere. The BVP solution can therefore be written as

$$\mathbf{u}(\psi)=\sum_{i=1}^{2N+2}\mathbf{u}^i(\psi)=\sum_{i=1}^{2N+2}\mathbf{U}^i(\psi)\cdot\boldsymbol{\alpha}^i=\sum_{i=1}^{2N+2}\sum_{\ell=1}^{2M}\alpha_\ell^i\mathbf{u}_\ell^i(\psi), \tag{30}$$

where $\mathbf{u}_\ell^i$ is the ℓ th mode on the i th subinterval and $\alpha_\ell^i\in C$ is the weight of this mode in the linear ODE's solution. As before, the ℓth mode $\mathbf{u}_\ell^i$ is identified by the index of its nonvanishing component at the rational surface abutting subinterval i. (For the first and last subintervals, which do not terminate on rational surfaces, $\mathbf{u}_\ell^1$ and $\mathbf{u}_\ell^{2N+2}$ are identified by their nonvanishing ℓth component at $\psi=0$ or $\psi=1$, respectively.) $\mathbf{U}^i(\psi)$ and $\boldsymbol{\alpha}^i$ represent the fundamental matrix of solutions and the coefficient vector, respectively, of subinterval i, which conveniently package these modes and their coefficients.

We note that the set $\{\alpha_\ell^i\}$ offers $(2N+2)\times(2M)$ DOF for the BVP solution. There are M boundary conditions imposed at each axis and edge, there are $(2M-2)$ continuity conditions imposed at each singular surface, and there are $2M$ conditions imposed on each "interstitial" surface that does not appear at a singular point, axis, or edge. This fixes $2\cdot M+(2M-2)\cdot N+(2M)\cdot(N+1)$ DOF, so that $2N$ more conditions are required to specify a BVP solution.

These remaining $2N$ DOF are specified in the most general way possible and comprise the information stored in the toroidal $2N\times 2N\,\Delta'$ matrix. We proceed to solve for Δ' as we did in the cylindrical case, by assigning a linearly independent set of values to the $2N$ coefficients associated with the $2N$ *big* solutions on each side of each singular surface. For every assignment of values, we solve the BVP and store in the Δ' matrix the resulting set of $2N$ *small* solution coefficients.

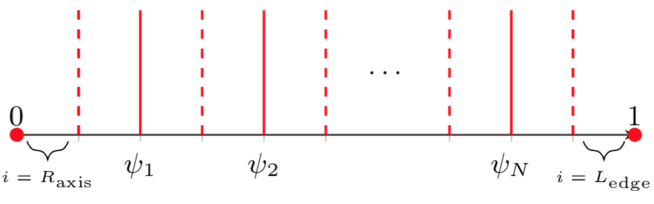

FIG. 1. This diagram models our interval setup for the toroidal geometry. Solid red lines represent singular surfaces (where continuity is imposed for the $2M-2$ nonresonant modes), while dashed lines represent "interstitial" nonsingular surfaces (where continuity is imposed for all $2M$ modes). The magnetic axis corresponds to $\psi=0$, while the plasma edge corresponds to $\psi=1$.

The toroidal definition of Δ' can therefore be written as

$$\Delta'_{ij}\equiv\left(\alpha^j_{s_j+M}\;\middle|\;\begin{array}{c}\alpha^k_{s_k}=\delta_{ik},\ \mathbf{q}(0)=\mathbf{q}(1)=0,\text{ and}\\ \text{all continuity conditions are satisfied}\end{array}\right), \tag{31}$$

where $i,j,k\in\{L_1,R_1,\ldots,L_N,R_N\}$ and s_j denotes the mode number of the big solution on interval j. (s_j+M denotes the corresponding small solution mode number.) We note that, because toroidal modes couple, the behavior of the big solution at any surface ψ_i may influence the behavior of the small solution at any other surface. Therefore, Δ' is no longer a diagonal matrix as it was in the cylindrical case.

We have therefore functionally defined Δ' as a mechanism to describe the relationships of the singular modes for all possible solutions of the BVP, thereby providing maximal flexibility to asymptotically match any model of the singular modes in the resistive inner region. In this sense, Δ' can be understood to represent the linear responses of small solutions to the "driving force" of the big solutions.[13] These resonant modes are most important in determining the behavior of the resistive layer.

The relationship of this matrix to the physics of tearing mode stability is no longer as clear as it was in the case of the slab or cylindrical model. For starters, this relationship depends on the inner region model that is used for the resistive layer. Furthermore, the coupling of modes in the toroidal geometry is what leads to the Δ' matrix being nondiagonal. A resonant perturbation at one surface of the plasma affects the resonant perturbations at every other rational surface due to their coupling with nonresonant modes which are everywhere continuous.

As a result, the Δ' matrix in toroidal geometry alone does not describe the equilibrium's tearing stability. The inner region equations must be matched against the information in Δ' to achieve a full picture. The matching procedure has been discussed at length in the previous literature,[10,19] and it is still an active area of research. However, this discussion past Δ' lies beyond the scope of this work.

III. CALCULATION OF Δ' IN A CYLINDRICAL EQUILIBRIUM

Having carefully defined in Sec. II the Δ' matrix in slab, cylindrical, and toroidal geometries, we now describe the numerical methods we have adapted to calculate Δ'. Before turning in Sec. IV to the numerical methods employed for the toroidal equilibrium, we first describe our calculation in a cylindrical geometry.

We assume a monotonic q profile, so that there exists only one singular surface for a given Fourier mode in the cylindrical plasma. We furthermore assume a pressureless plasma, so that the asymptotic expansions in Eq. (17) are valid. (This limitation is by no means necessary but is useful for ease of presentation.) Our procedure for generating Δ' then proceeds as follows:

1. Form the 2×2 fundamental matrices of solutions—$\mathbf{X}_L(s=-\epsilon)$ and $\mathbf{X}_R(s=+\epsilon)$—on each side of the singular surface, initialized with the linearly independent set of asymptotic expansions in Eq. (17)

$$\mathbf{X}_{R,L}(\pm\epsilon) \equiv \begin{pmatrix} \psi_B(\pm\epsilon) & \psi_S(\pm\epsilon) \\ \psi_B'(\pm\epsilon) & \psi_S'(\pm\epsilon) \end{pmatrix} \approx \begin{pmatrix} 1 & \pm\epsilon \\ \kappa \ln|\epsilon| & 1 \end{pmatrix}. \tag{32}$$

2. "Shoot" these fundamental matrices from the singular surface to the profile boundaries by integrating the ODE in Eq. (12), mapping $\mathbf{X}_L(s=-\epsilon)$ to $\mathbf{X}_L(r=0)$ and $\mathbf{X}_R(s=\epsilon)$ to $\mathbf{X}_R(r=2a)$.
3. Leveraging the linearity of the ODE, find the linear combination of columns of $\mathbf{X}_L(0)$ and $\mathbf{X}_R(2a)$ necessary to satisfy the boundary conditions $\psi(0)=\psi(2a)=0$.
4. Scale the resulting coefficients to set the first column's (i.e., the big solution's) coefficient to 1 and store the second column's (the small solution's) coefficients in the Δ' matrix.

Note that only one shot is required (on each side of the singular surface) in which the big solution coefficient is set to 1 because the independence of solutions in the two regions of the cylindrical model renders all other choices for the big solution coefficient trivial.

In Figs. 2 and 3, we compare the results of the above method against the results of Refs. 3 and 4, adopting these references' definition of Δ'. In particular, these plots define $\Delta' = (A_R - A_L)$, the difference of the small coefficients on the diagonal of our Δ' matrix, as defined in Eq. (21). We find that we replicate previous results despite our modifications to the solution method.

The helpfulness of shooting asymptotic solutions away from the singular surfaces is evident upon inspection of the expansions in Eq. (32). In particular, we note that, despite

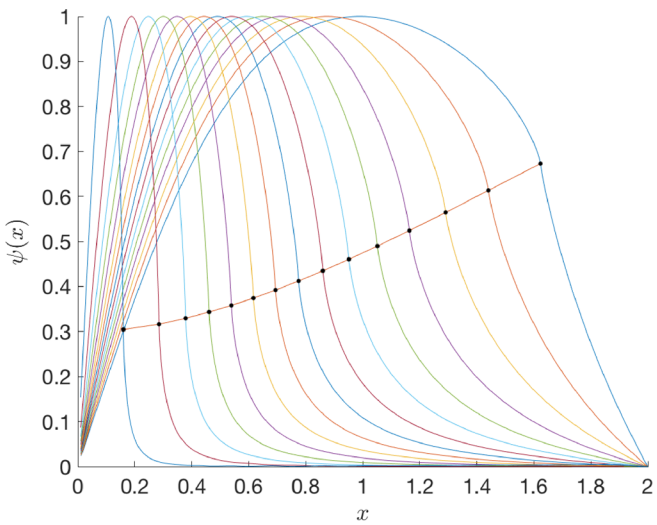

FIG. 2. This chart depicts $m/n = 2/1$, $a/R_0 = 0.05$ solutions to the cylindrical Newcomb equation (12) for a magnetic perturbation ψ, scanned over an increasingly pitch-angled q profile: $q(x) = q_0(1+x^2)$. The location of the singular surface (noted by a dot for each scan) moves inward as q_0 increases. $x \equiv \frac{r}{a}$ is a dimensionless radial coordinate. This chart matches that in Fig. 1(a) of Ref. 3 and Fig. 1 of Ref. 4.

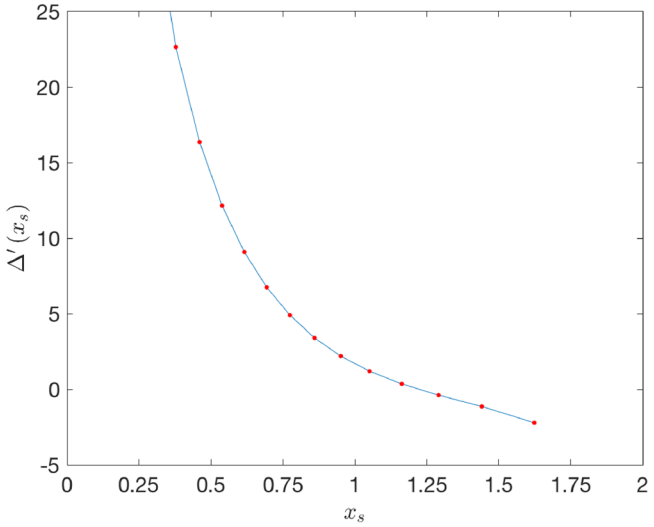

FIG. 3. A chart of Δ' values achieved over the same equilibrium scan as Fig. 2, depicting increasingly RMHD-unstable ($\Delta' > 0$) equilibria as q_0 increases. This chart matches that in Fig. 1(b) of Ref. 3 and Fig. 2 of Ref. 4.

their disparate behavior near the singularity, the two modes approximate the solution subspace $\binom{0}{1}$ as $\epsilon \to 0$. When integrating any mode that has a nonzero projection along the big solution, therefore, this projection can grow to dominate the mode upon the approach to the singular surface. Similarly, for modes that have any projection along the small solution, such a projection can dominate the solution when integrated away from the singular surface. To maintain the linear independence of two different modes, therefore, it is more reliable numerically to explicitly "pick out" the big and small solutions, which remain independent as they are integrated away from the singularity.

By implementing the fundamental matrix technique of Ref. 1 and adopting the "shooting *away*" method of *Nishimura et al.*[3] (while avoiding the slowness and cycling of Newton's iteration), we have thus developed a more robust method for Δ' calculation in the cylinder.

IV. CALCULATION OF Δ' IN A 2D TOROIDAL EQUILIBRIUM

We now describe the numerical methods of `STRIDE` for the calculation of Δ' in a toroidal geometry. The cylindrical solution methods of Sec. III anticipate the most salient features of our toroidal calculation. However, we must organize the toroidal calculation to account for the many simultaneous constraints of the new geometry.

The toroidal Δ' matrix is constructed from solutions to the ODE of Eq. (24). In particular, we use Eq. (24) to define a BVP with boundary and continuity conditions given by Eq. (29). We then solve this BVP as follows:

1. On each side of every singular surface ψ_i, we initialize at $\psi_i \pm \epsilon$ a fundamental matrix of solutions whose columns are comprised by the asymptotic expansions described in Eqs. (26)–(28)

$$\mathbf{U}^{L_i}(\psi_i-\epsilon)\equiv\mathbf{\Phi}(\psi_i^-,\psi_i^-)\quad\text{and}\qquad \mathbf{U}^{R_i}(\psi_i+\epsilon)\equiv\mathbf{\Phi}(\psi_i^+,\psi_i^+). \tag{33}$$

We use the notation $\psi_i^{\pm}\equiv\psi_i\pm\epsilon$, and let $\mathbf{\Phi}(\psi_B,\psi_A)$ represent the propagator of the ODE from $\psi=\psi_A$ to $\psi=\psi_B$, a fundamental matrix of solutions as described in Ref. 1. [The notation $\mathbf{U}^i(\psi)$ was introduced in the discussion following Eq. (30).]

2. At the magnetic axis and plasma edge, we further initialize fundamental matrices of modes which span the subspace of solutions consistent with the boundary conditions, $\mathbf{q}(0)=\mathbf{q}(1)=0$. We denote these fundamental matrices by $\mathbf{\Phi}(0,0)$ and $\mathbf{\Phi}(1,1)$. They are $2M\times M$ matrices which take the form

$$\mathbf{\Phi}(0,0)=\mathbf{\Phi}(1,1)=\begin{pmatrix}0_M\\1_M\end{pmatrix}. \tag{34}$$

3. By integrating Eq. (24), we "shoot" each initialized fundamental matrix across its interval, ending at the interval's "interstitial" surface, which we label as a_i. We denote by $\mathbf{\Phi}(a_{i-1},\psi_i^-)$, for example, the $2M\times 2M$ fundamental matrix initialized at $(\psi_i-\epsilon)$ with the asymptotic expansion $\mathbf{\Phi}(\psi_i^-,\psi_i^-)$ and propagated backward toward a_{i-1} (see Fig. 4).
4. Continuity in all $2M$ modes is imposed at interstitial surfaces by demanding, for example, that

$$\mathbf{\Phi}(a_i,\psi_i^+)\cdot\boldsymbol{\alpha}^{R_i}=\mathbf{\Phi}(a_i,\psi_{i+1}^-)\cdot\boldsymbol{\alpha}^{L_{i+1}}. \tag{35}$$

As introduced in Eq. (30), $\boldsymbol{\alpha}^i\in C^{2M}$ represents the coefficients weighting each mode in subinterval i.

5. Continuity in $2M-2$ modes is imposed at each rational surface simply by demanding that

$$\alpha_\ell^{L_i}=\alpha_\ell^{R_i} \tag{36}$$

for each mode $\ell\notin\{s_{L_i},s_{L_i}+M\}=\{s_{R_i},s_{R_i}+M\}$. The simplicity of this continuity condition is the result of the fact that, as discussed after Eq. (28), the asymptotic expansions stand in for the integration of modes which, at $\psi=\psi_i$, form the matrix columns of Eq. (28). In effect, the expansions serve as maps which preserve the identities of the modes born at the singular surface.

6. These conditions are solved simultaneously by forming them into a sparse matrix representation of the BVP, as in Eq. (37).
7. This sparse matrix equation is solved $2N$ times, with each linearly independent assignment of big solution coefficients. The resulting small solution coefficients are stored in the Δ' matrix.

For ease of exposition, we explicitly notate the sparse matrix equation for an $(N=2)$-singular-surface problem, but the construction easily generalizes to an arbitrary number of surfaces. We let $\boldsymbol{\alpha}^i$ represent the second half of the $2M$ mode coefficients on interval i: $\{\alpha^i_{M+1},\ldots,\alpha^i_{2M}\}$. [This subset of coefficients is needed on the first and last intervals, on which only half of the $2M$ modes satisfy the boundary conditions $\mathbf{q}(0)=\mathbf{q}(1)=0$.] To enforce continuity in all nonresonant modes at singular surfaces, we denote by $1^{s_i}_{s_i+M}$ the $(2M-2)\times 2M$ matrix formed by deleting rows $\{s_i,s_i+M\}$ of the identity matrix 1_{2M}. Finally, we denote by 1_{s_i} the $1\times 2M$ row vector for which the only nonzero entry is 1 in the s_ith component—the "big solution" component at ψ_i.

Thus, we may write our BVP as

$$\begin{array}{c|cccccc}
 & M & 2M & 2M & 2M & 2M & M\\
2M & \mathbf{\Phi}(a_0,0) & \mathbf{\Phi}(a_0,\psi_1^-) & & & & \\
2M-2 & & -\mathbb{1}^{s_1}_{s_1+M} & \mathbb{1}^{s_1}_{s_1+M} & & & \\
2M & & & -\mathbf{\Phi}(a_1,\psi_1^+) & \mathbf{\Phi}(a_1,\psi_2^-) & & \\
2M-2 & & & & -\mathbb{1}^{s_2}_{s_2+M} & \mathbb{1}^{s_2}_{s_2+M} & \\
2M & & & & & -\mathbf{\Phi}(a_2,\psi_2^+) & \mathbf{\Phi}(a_2,1)\\
1 & & 1_{s_1} & & & & \\
1 & & & 1_{s_1} & & & \\
1 & & & & 1_{s_2} & & \\
1 & & & & & 1_{s_2} &
\end{array}
\cdot
\begin{pmatrix}\boldsymbol{\alpha}^{R_{\text{axis}}}\\ \boldsymbol{\alpha}^{L_1}\\ \boldsymbol{\alpha}^{R_1}\\ \boldsymbol{\alpha}^{L_2}\\ \boldsymbol{\alpha}^{R_2}\\ \boldsymbol{\alpha}^{L_{\text{edge}}}\end{pmatrix}
=
\begin{pmatrix}0\\0\\0\\0\\0\\ \begin{bmatrix}1\\0\\0\\0\end{bmatrix}\end{pmatrix}. \tag{37}$$

We have notated the number of rows and columns in each block.

Each block row of this matrix equation represents a set of continuity criteria at the interface of two intervals, and the last four rows represent the assignment of big solution coefficients. The bracketed vector in the RHS of Eq. (37) represents a case when the big solution on L_1 is assigned a coefficient of 1, and the remaining big solution coefficients are set to 0. This setting must be permuted to span all linearly independent cases, and the BVP must therefore be solved four times with varying RHS. In the above example, a row of the resulting $4\times 4\,\Delta'$ matrix would be composed of the solved-for small solution coefficients: $\{\alpha^{L_1}_{s_{L_1}+M},\ \alpha^{R_1}_{s_{R_1}+M},\ \alpha^{L_2}_{s_{L_2}+M},\alpha^{R_2}_{s_{R_2}+M}\}$.

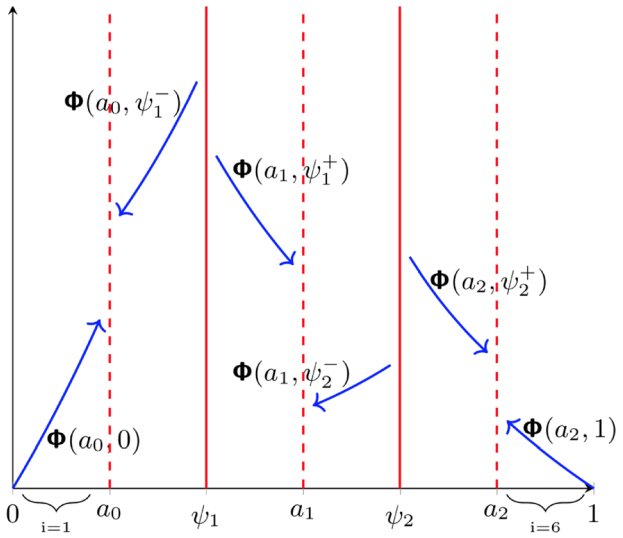

FIG. 4. A schematic of the propagators $\mathbf{\Phi}(\cdot,\cdot)$ for an equilibrium with $N=2$ rational surfaces, initialized at the axis, at the edge, and at $\psi_i^{\pm} \equiv \psi_i \pm \epsilon$ for all singular ψ_i. These propagators are "shot" across their subintervals by integrating the ODE Eq. (24) forward *and* backward, as appropriate. The final state of these propagators, whose columns are the final values of the integrated modes at the "interstitial" surfaces a_i, is then used to construct the sparse matrix representation of the BVP, Eq. (37).

This sparse matrix BVP solution is made possible by the linearity of the ideal MHD ODE—Eq. (24)—that we solve in the external regions. Asymptotic expansions at singular points of the ODE, and the abundant use of state transition matrices to subdivide the integration interval and enforce continuity conditions, provide a robust solution for the calculation of Δ' in toroidal geometry.

We also note that the ideal-wall boundary condition for Δ'—specified in step 2 of the above procedure—is not the only possible choice. In particular, given a vacuum response matrix $\mathbf{W_V}$ from a code such as VACUUM,[20,21] the choice of the plasma edge boundary condition

$$\mathbf{\Phi}(1,1) = \begin{pmatrix} 1_M \\ -\mathbf{W_V} \end{pmatrix} \tag{38}$$

solves for the Δ' matrix consistent with the total minimization of plasma and vacuum energy, δW, as described in Eq. (6) of Ref. 5.

We compare the results of our `STRIDE` code with those of resistive DCON[5] using DIII-D equilibria reconstructions generated by EFIT[22] and CAKE,[23] respectively—the latter of which is a fast kinetic equilibrium solver currently under development and intended for real-time stability calculations. In so doing, we bootstrap resistive DCON's own benchmarking against various resistive MHD codes, including the MARS[9] and PEST[24,25] codes. In cases when data are available from both the `STRIDE` code and resistive DCON, Figs. 5 and 6 demonstrate strong agreement on the values of Δ', particularly for low-q surfaces within the plasma.

V. NUMERICAL ADVANTAGES AND RESULTS OF THE `STRIDE` CODE

For many years, the numerical challenge of the Δ' BVP has been approached by finite element Galerkin methods.[5,11–13] The Galerkin discretization of elliptic partial differential equations (PDEs) is a variational method that recasts a PDE in its weak form—in particular as a bilinear form which must be minimized by solving for a weighting of

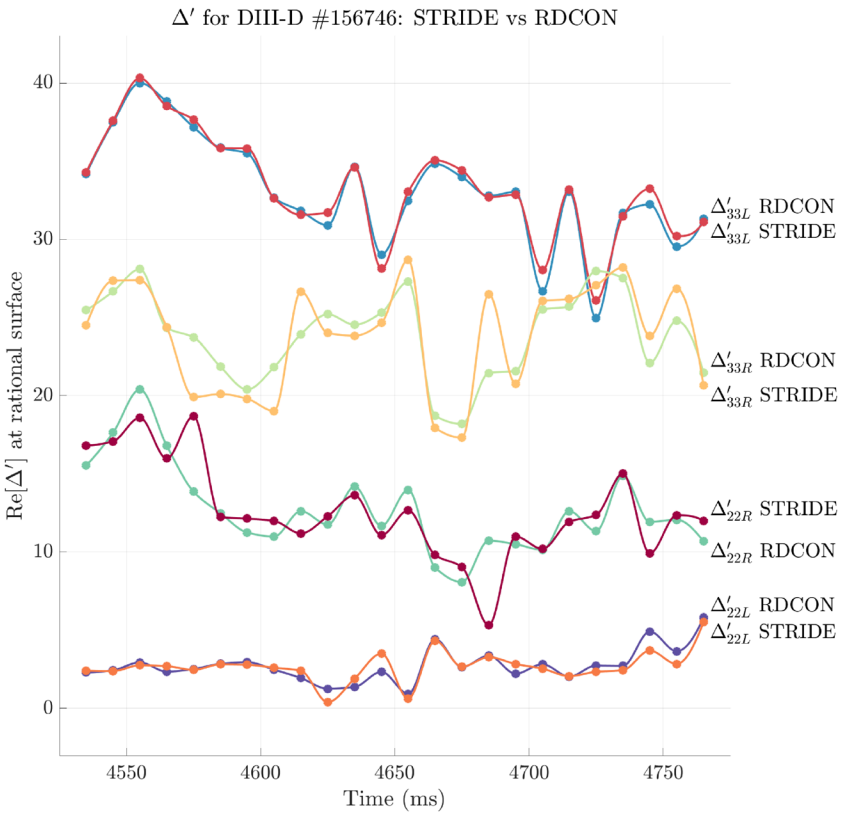

FIG. 5. This chart depicts $\mathrm{Re}[\mathrm{diag}(\Delta')]$, the real part of the Δ' matrix diagonal, for $q=2$ and $q=3$ surfaces of an EFIT[22] reconstruction for DIII-D shot #156746. It reveals strong agreement between resistive DCON and the new state transition matrix code, STRIDE. Notationally, the time trace Δ'_{22L} denotes the real part of the Δ' diagonal element corresponding to the left side of the $q=2$ surface. The Δ' BVP was solved for this chart with the assumption of an ideal wall at the plasma edge.

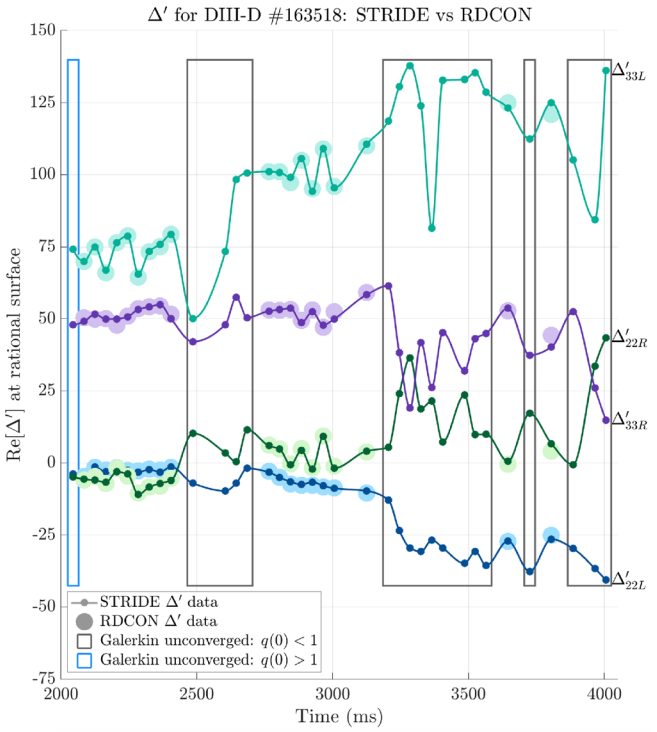

FIG. 6. These time traces depict Re[diag(Δ′)] for low-q surfaces of CAKE[23] equilibrium reconstructions over several timeslices of DIII-D shot #163518. Sections of the data are emphasized in which the STRIDE code successfully generated the Δ′ matrix, while the Galerkin method did not converge. In this shot, such divergences occur for the most part when $q(0) < 1$. Over half of the $q(0) < 1$ cases above are, as measured by the Newcomb criterion,[2] unstable to ideal MHD $m = 1$ internal kink modes as well.

discrete basis functions. The existence and uniqueness of solutions for this minimization are dependent on the bilinear form, satisfying a positive-definiteness requirement. In modern treatments, this positive-definiteness is referred to as the *coercivity* of the bilinear form.[26]

As discussed in Ref. 12, the Galerkin discretization of the cylindrical ideal MHD Newcomb equation[16] employs a bilinear form that measures the plasma response energy $W(u, u)$ of a magnetic perturbation u

$$W(u,v) \equiv \int_0^1 \left(fu'v' + guv\right)\mathrm{d}r. \tag{39}$$

As defined, however, the bilinear form W is only positive-definite for ideal-MHD-*stable* equilibria. The Galerkin discretization of the cylindrical Newcomb equation—as formulated in Ref. 12—therefore, is not guaranteed to produce a solution for ideal-MHD-unstable equilibria. Resistive DCON's Galerkin formulation draws from a comparable Galerkin discretization, so that its solution for Δ′ in ideal-MHD-unstable equilibria is similarly susceptible.

In Fig. 6, we display matrix elements of Δ′ over several time slices of DIII-D shot #163518, as measured by STRIDE and resistive DCON. For most data points, the two codes show strong agreement. In this particular shot, however, for equilibria with a $q = 1$ surface, the direct integration approach of STRIDE converges, while the Galerkin approach does not. Most of the equilibria with $q(0) < 1$ in Fig. 6 are also ideal-MHD-unstable, as determined by the Newcomb criterion.[2]

Unlike the *weak* form of the Galerkin method, STRIDE solves the perturbed ideal MHD equations in their *strong* form—directly integrating the matrix Newcomb Eq. (22). Numerical experimentation has demonstrated that STRIDE has comparable ease solving for Δ′ in the presence of a $q = 1$ surface or in an ideal-MHD-unstable equilibrium as it does in better-conditioned equilibria. The wide applicability of STRIDE is useful in several contexts:

1. it affords a robust tearing stability analysis for ITER, where some operation conditions are expected to have $q(0) < 1$;
2. although it bears noting that Eq. (22) is itself derived assuming ideal MHD stability (i.e., $\omega\tau_A \ll 1$), STRIDE still affords an effective time-series analysis of tearing stability during tokamak shots that exhibit ideal MHD instabilities which nonlinearly saturate—e.g., sawtooth oscillations; and
3. it enables a high-throughput real-time stability analysis that is robust to measurement error, as required in a control algorithm.

In addition to its improved robustness, the STRIDE's state transition matrix method affords an immediate parallelization of the ideal MHD ODE integration, as described in Eq. (29) of Ref. 1. In particular, each subinterval depicted in Fig. 4 may be *further* subdivided—as finely as desired—with each subdivision integrated in parallel. The state transition matrices independently integrated on each subinterval can then be multiplied together to *propagate* the ODE solution across the interval. For example, this subdivision takes the form

$$\mathbf{x}(\psi_2) = \mathbf{\Phi}(\psi_2,\psi_0)\mathbf{x}(\psi_0) = \mathbf{\Phi}(\psi_2,\psi_1)\mathbf{\Phi}(\psi_1,\psi_0)\mathbf{x}(\psi_0), \tag{40}$$

where the columns of $\mathbf{\Phi}$ comprise linearly independent ODE solutions, as above. In general, the calculation time for such matrix multiplication considerably outpaces the numerical integration it replaces.

We note that the parallel integration of intervals in the manner described above scales with the availability of additional processors. Although more work can further reduce thread overhead, Fig. 7 depicts the significant reduction in solution time achieved by an initial parallel implementation of STRIDE, with a fastest run-time under 500 ms. STRIDE integrates using the complex adaptive integrator ZVODE,[27] whose accuracy is tunable up to machine precision.

We surmise that additional gains in computation speed would follow from further optimizing analytical features of our code. For example, the self-adjointness of the ideal MHD force operator may be exploited to reduce the computational burden of ODE integration. In particular, the reciprocity relations of the Δ′ matrix discussed in Refs. 13 and 28 could reduce the degrees of freedom of the Δ′ BVP. Similarly, the square-root algorithm[29] for Riccati problems could reduce the computational burden of ODE integration for a Riccati formulation[1] of the self-adjoint ideal MHD problem.

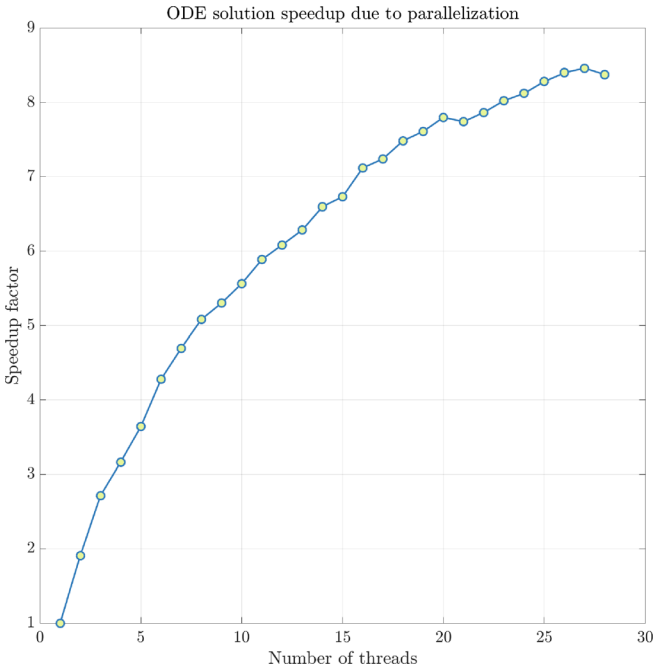

FIG. 7. The state transition matrix method allows for a parallelized BVP solution of Δ'. The plot above depicts the speedup achieved with the increased threadcount for the solution of the Δ' matrix BVP. The fastest speedup above corresponds to an ODE solution time of 415 ms.

As a final remark, we note that the matrix (represented for the $N=2$ case) in Eq. (37) has a reliable sparsity pattern that may enable specialized sparse matrix solutions. Such enhancements are less important for tokamak equilibria, whose modes are uncoupled across toroidal mode numbers n (and which therefore have comparatively small matrices to solve). However, tearing mode analysis in stellarator equilibria may benefit from attention to this feature.

VI. SUMMARY AND CONCLUSION

We have introduced STRIDE, a robust and effective code to solve the intractable Δ' boundary value problem. In our presentation of this solution, we have reviewed at length the definition of Δ' in the slab, cylindrical, and toroidal geometries and emphasized the varying role Δ' plays in determining tearing stability.

We believe that, due to the speed and robustness of its state transition matrix methods, STRIDE substantially improves upon previously known solution methods for Δ'. We have demonstrated that the numerical techniques of Ref. 1—developed for the parallel solution of *ideal* MHD equations—are sufficiently flexible to resolve the asymptotic expansions necessary for Δ' *resistive* MHD calculations. We have also emphasized an interpretation of linear ODE asymptotic expansions as substituting for *integration* over small intervals that terminate on singular points; this profitable point of view helps illuminate how such expansions are to be used in ODE solutions.

We have favorably benchmarked the STRIDE's state transition matrix method against previous well-established solutions for Δ' in both cylindrical and toroidal geometries. STRIDE has demonstrated accuracy in all our tests.

To expand the scope of applicability of our work, further effort is also required to improve the reliability of asymptotic expansions near rational surfaces in low-β plasmas. Such improvements would likely enable more accurate tearing stability analysis in the high-q edge regions of tokamak equilibria.

With a BVP solution time of less than 500 ms, we hope that our efforts help enable future active feedback methods for control of tokamak plasmas. Alongside fast equilibrium reconstruction tools such as CAKE,[23] this work helps demonstrate the numerical feasibility of solving challenging ideal and resistive MHD stability analyses in a timescale comparable to the tokamak's stable equilibrium evolution time and for a wider class of equilibria than previously achieved.

ACKNOWLEDGMENTS

We would like to thank Zhirui Wang and Alan Glasser for many helpful conversations and suggestions. We would also like to thank David Eldon and Matthijs Roelofs for making the CAKE data available and Steven Sabbagh for making the NSTX data available. This research was supported in part by the U.S. Department of Energy (DoE) under Contract No. DE-AC02-09CH11466 and the DoE Early Career Research Program: No. DE-SC0015878.

[1]A. S. Glasser, E. Kolemen, and A. H. Glasser, "A Riccati solution for the ideal MHD plasma response with applications to real-time stability control," Phys. Plasmas **25**(3), 032507 (2018).
[2]A. H. Glasser, "The direct criterion of Newcomb for the ideal MHD stability of an axisymmetric toroidal plasma," Phys. Plasmas **23**, 072505 (2016).
[3]Y. Nishimura, J. D. Callen, and C. C. Hegna, "Tearing mode analysis in tokamaks, revisited," Phys. Plasmas **5**, 4292–4299 (1998).
[4]H. P. Furth, P. H. Rutherford, and H. Selberg, "Tearing mode in the cylindrical tokamak," Phys. Fluids **16**, 1054 (1973).
[5]A. H. Glasser, Z. R. Wang, and J.-K. Park, "Computation of resistive instabilities by matched asymptotic expansions," Phys. Plasmas **23**, 112506 (2016).
[6]O. Sauter, M. A. Henderson, G. Ramponi, H. Zohm, and C. Zucca, "On the requirements to control neoclassical tearing modes in burning plasmas," Plasma Phys. Controlled Fusion **52**, 025002 (2010).
[7]F. Turco and T. Luce, "Impact of the current profile evolution on tearing stability of ITER demonstration discharges in DIII-D," Nucl. Fusion **50**, 095010 (2010).
[8]H. P. Furth, J. Killeen, and M. N. Rosenbluth, "Finite-resistivity instabilities of a sheet pinch," Phys. Fluids **6**, 459 (1963).
[9]A. Bondeson, G. Vlad, and H. Lütjens, "Resistive toroidal stability of internal kink modes in circular and shaped tokamaks," Phys. Fluids B: Plasma Phys. **4**, 1889–1900 (1992).
[10]A. H. Glasser, J. M. Greene, and J. L. Johnson, "Resistive instabilities in general toroidal plasma configurations," Phys. Fluids **18**, 875 (1975).
[11]R. C. Grimm, R. L. Dewar, and J. Manickam, "Ideal MHD stability calculations in axisymmetric toroidal coordinate systems," J. Comput. Phys. **49**, 94–117 (1983).
[12]A. D. Miller and R. L. Dewar, "Galerkin method for differential equations with regular singular points," J. Comput. Phys. **66**, 356–390 (1986).
[13]A. Pletzer and R. L. Dewar, "Non-ideal stability: Variational method for the determination of the outer-region matching data," J. Plasma Phys. **45**, 427 (1991).
[14]G. Vlad and A. Bondeson, "Numerical simulations of sawteeth in tokamaks," Nucl. Fusion **29**, 1139 (1989).
[15]R. J. Goldston, in *Introduction to Plasma Physics*, edited by P. H. Rutherford (Institute of Physics Publishing, Philadelphia, 1995), Chap. 20.
[16]W. A. Newcomb, "Hydromagnetic stability of a diffuse linear pinch," Ann. Phys. **10**, 232–267 (1960).

[17]H. L. Turrittin, "Convergent solutions of ordinary linear homogeneous differential equations in the neighborhood of an irregular singular point," Acta Math. **93**, 27–66 (1955).
[18]C. Mercier, "Un critère necéssaire de stabilité hydromagnetique pour un plasma en symétrie de révolution," Nucl. Fusion **1**, 47 (1960).
[19]A. H. Glasser, S. C. Jardin, and G. Tesauro, "Numerical solution of the resistive magnetohydrodynamic boundary layer equations," Phys. Fluids **27**, 1225 (1984).
[20]M. Chance, "Vacuum calculations in azimuthally symmetric geometry," Phys. Plasmas **4**, 2161–2180 (1997).
[21]M. Chance, A. Turnbull, and P. Snyder, "Calculation of the vacuum Greens function valid even for high toroidal mode numbers in tokamaks," J. Comput. Phys. **221**, 330–348 (2007).
[22]L. L. Lao, H. S. John, R. D. Stambaugh, A. G. Kellman, and W. Pfeiffer, "Reconstruction of current profile parameters and plasma shapes in tokamaks," Nucl. Fusion **25**, 1611 (1985).
[23]D. Eldon, E. Kolemen, M. A. Roelofs, W. J. Eggert, A. S. Glasser, N. C. Logan, D. A. Humphreys, O. Meneghini, and S. P. Smith, "Development of an automatic kinetic equilibrium reconstruction workflow for tokamak plasma stability analysis" (unpublished).
[24]R. L. Dewar and A. Pletzer, "Two-dimensional generalizations of the Newcomb equation," J. Plasma Phys. **43**, 291 (1990).
[25]A. Pletzer, A. Bondeson, and R. L. Dewar, "Linear stability of resistive MHD modes: Axisymmetric toroidal computation of the outer region matching data," J. Comput. Phys. **115**, 530–549 (1994).
[26]S. C. Brenner and L. R. Scott, *The Mathematical Theory of Finite Element Methods*, Texts in Applied Mathematics Vol. 15, 3rd ed. (Springer, New York, NY, 2008).
[27]A. C. Hindmarsh, in *ODEPACK, A Systematized Collection of ODE Solvers*, edited by R. Stepleman (North-Holland Publishing, Amsterdam, 1983).
[28]R. L. Dewar and M. Persson, "Coupled tearing modes in plasmas with differential rotation," Phys. Fluids B: Plasma Phys. **5**, 4273–4286 (1993).
[29]R. F. Stengel, *Optimal Control and Estimation* (Dover Publications, Inc., New York, 1994).